CHAPTER 7

MORPHOLOGY OF LARGE-SCALE PRECIPITATING WEATHER SYSTEMS

7.1 <u>Introduction</u>. The character of precipitation is largely controlled by vertical air motions, static stability, horizontal kinematics (e.g., deformation and vorticity), and shear of the horizontal winds in the vertical. Radar observations of the aerial extent, intensity, and lifetime of precipitation systems are evidence of the physical processes at work in the atmosphere. Depending on the dominant mechanism responsible for the vertical air motion, precipitation is usually classified into one of these two types:

Stratiform - Widespread, continuous precipitation produced by large-scale ascent due to warm advection, positive vorticity advection, deformation, frontagenessis, topographical lifting, or large-scale horizontal air convergence caused by other means.

Convective - Localized, rapidly changing, showery precipitation produced by cumulus-scale convection in unstable or conditionally unstable air.

The distinction between stratiform and convective precipitation is not always clear in practice. Widespread precipitation, for example, is often accompanied by fine-scale structures, or embedded convective elements. In fact, precipitation systems generally are composed of a broad spectrum of vertical motion scales and intensities. Nevertheless, it is usually possible to classify precipitation patterns by their dominant scale.

7.1.1 Stratiform Rain and Snow. Stratiform precipitation is most often produced in nimbostratus clouds or cumulus cloud shields such as those with Mesoscale Convective Systems (MCSs) or in the cold sectors northwest through east of warm fronts and ExtraTropical Cyclone (ETC) centers. Upward air motions are relatively weak (a few cm s^{-1} to a few ms^{-1}) and the vertical structure of the reflectivity pattern is closely related to the precipitation growth process during gravitational settling.

The presence of stratiform precipitation facilitates wind measurements with the Velocity Azimuth Display (VAD) technique and the VAD Wind Profile (VWP) products (Chapter 6) to much higher altitudes than possible in clear air. The wind profiles observed during precipitation are useful in determining the nature of thermal advection, jets, slantwise flow, fronts, accuracy of numerical models, etc.

On most occasions, mesoscale precipitation bands form not only along boundaries such as fronts but also within the stratiform precipitation area of ETCs. These bands arise from warm advection, local slantwise vertical motion, deformation zones, gravity waves, as well as variable instabilities and wind shears generated within large-scale systems. Such a mesoscale band within a larger precipitation echo is shown in Figure 7-1. The band is within a cold frontal region. Other bands have different orientations with respect to the shear profiles and zones of deformation. Bands also occur in the vicinity of and north of warm frontal zones. Embedded convective regions are also common in these same precipitation regions.

7.1.2 Bright Band. Apparently the bright band was first documented by the Canadian Army Operational Research Group during WW II (Atlas 1990). It was notably absent within convective storms. In stratiform precipitation where lower portions of the echo are at or above freezing temperatures and higher levels are below freezing, a thin layer of relatively high reflectivity (bright band) is often observed just below the level of 0° C in the phase transition region (Figure 7-2). As snowflakes descend into this layer they become wet and begin to coalesce developing larger, wet flakes of snow that begin to melt and coalesce still further. This highly reflective mixture warms still further and changes completely into rain. The radar reflectivity of the large, wet snowflakes is up to 15 dB higher, principally because of their large size and because the dielectric constant of water (0.93) exceeds that of ice (0.19) by a factor of nearly five. Descending further below the bright band, the raindrops accelerate their fall speed (to 5 ms^{-1}) exceeding the fall-speed of snowflakes (1.3 ms^{-1}) above resulting in a diminished hydrometeor concentration. This decrease in size and number of hydrometeors accounts for the lower reflectivity just below the bright band. Table 7-1 summarizes the physical causes of bright bands by accounting for the changes in backscatter echo intensity.

Table 7-1
Average Echo Intensity Change (dB) Due to
Physical Factors Above and Below the Bright Band

	Dielectric	Fall Velocity	Coalescence	Shape	Growth	Total
Snow to bright band	+4	-1.5	+3	+1.5	0	+7
Bright band to rain	+1	-5.5	-1	-1.5	0.5	-6.5

Figure 7-2 is an example of a bright band within generally stratiform precipitation.

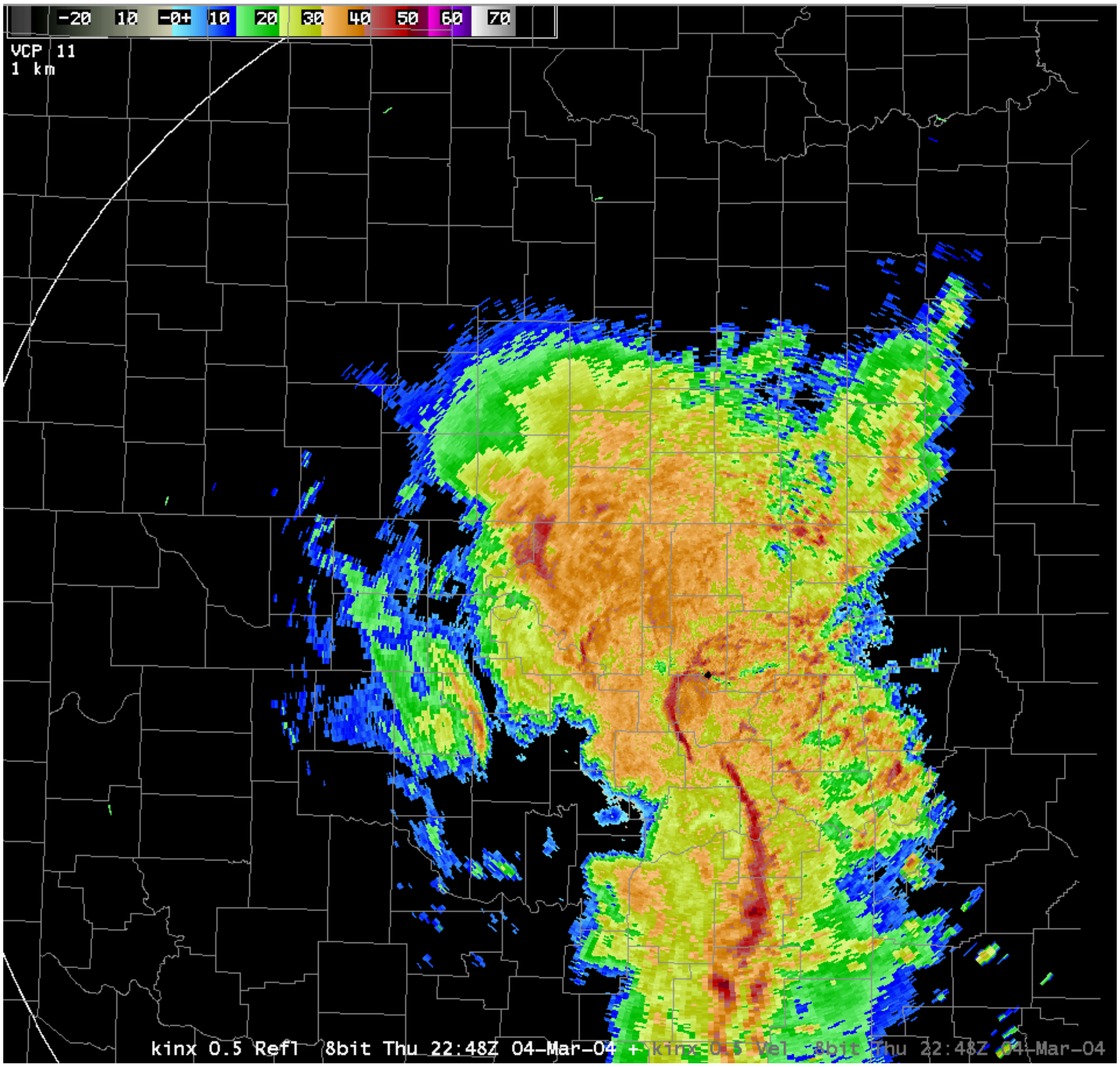

Figure 7-1
Precipitation Band Along a Cold Front Within an ETC

Tulsa, OK WSR-88D Reflectivity Data Array product at 22:48 UTC on 4 March 2004 (AWIPS display). The mesoscale precipitation band is along a cold front extending southward from the surface circulation center located about 80 nm (148 km) north northwest of the radar.

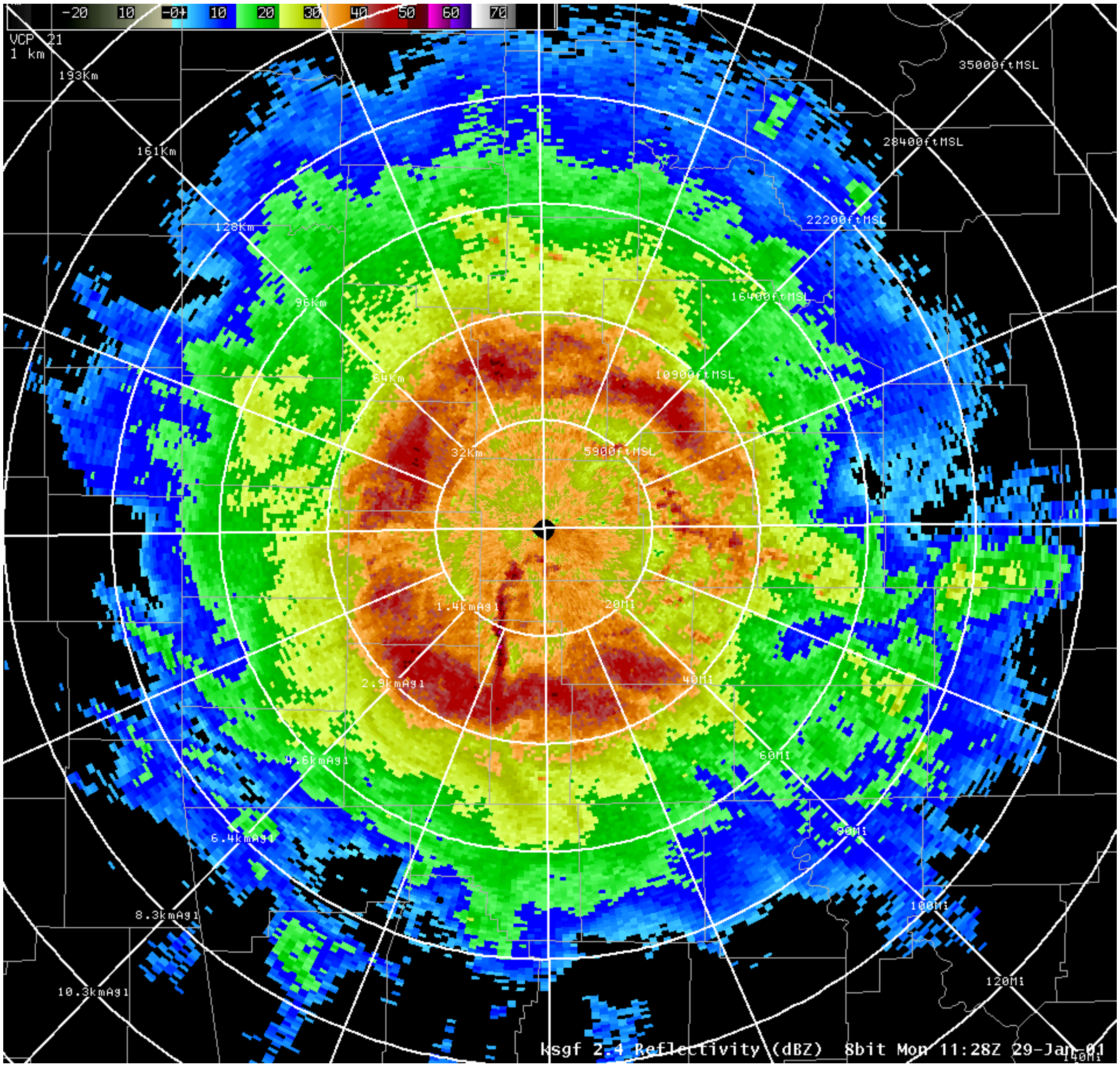

Figure 7-2
Bright Band

Springfield, MO WSR-88D Reflectivity Data Array product at 11:28 UTC on 29 January 2003 (AWIPS display). Note the bright band reflectivity varies from ~ 35 dBZ to 50 dBZ and the height averages ~ 9000 ft (2700 m). A nearby sounding indicated the environmental freezing level at 9440 ft (2877 m).

7.2 <u>Mesoscale Convective Systems</u>. Some large-scale precipitating systems begin as combinations of a number of convective elements. The resulting system, although still feeding on unstable air, takes on a character much different from typical cumulus-scale convection yet it can still be considered a multicell system. Regions of strong convection and heavy showers can become distributed in bands within a larger area of developing stratiform precipitation or the strong convection can be limited to the large system's leading edge with the rest of the system primarily composed of stratiform rain. However, the convective line can, at times, be near the trailing edge as well. When organized in a linear fashion, the multicell convective elements are typically distributed along a band about 20 km (11 nm) wide and hundreds of kilometers long. The bands are related to the low-level "cold pool," convergence, both low-level and deep layer wind flow and shear, the Earth's topography, and the rotation of elements within the line itself can all affect the structure of the rain areas. The characteristics of precipitation bands have been categorized, but it is not completely understood why precipitation has the strong tendency to become organized into the characteristic scales and patterns that are observed.

Precipitation areas can be grouped into categories of size and lifetime. Observations show that synoptic areas that are larger than 10^4 km^2 (2915 nm^2) have lifetimes of one day or longer; large mesoscale areas that range from 10^3 to 10^4 km^2 (291 to 2915 nm^2) last several hours; small mesoscale areas that cover 100 to 400 km^2 (29 to 116 nm^2) last about an hour; and elements that are about 10 km^2 (2.9 nm^2) in size usually last no longer than half an hour. Along with the larger mesoscale features, typically the smaller deep moist convective elements have the highest rain rates and supply the major contribution to the total rainfall.

Multicell storms are a common occurrence when deep, moist, convection organizes in clusters, lines, or areas. Multicells are defined in this text as a group of cells in close proximity sharing a common cold pool and precipitation area. In Maddox's (1980) classification of the Mesoscale Convective Complex (MCC), multicells could be thought of as belonging to both Linear and Circular types (Figure 7-3).

The term Mesoscale Convective System (MCS) (Zipser 1982) includes all precipitation systems 20 to 500 km (11 to 270 nm) wide that contain deep convection. Examples in middle-latitudes are large isolated thunderstorms, squall lines, MCCs, and rain bands. The aerial extent of these systems is often too large to be covered by a single radar. Examination of mosaic maps from a network of radars is required to capture the full extent of many MCSs.

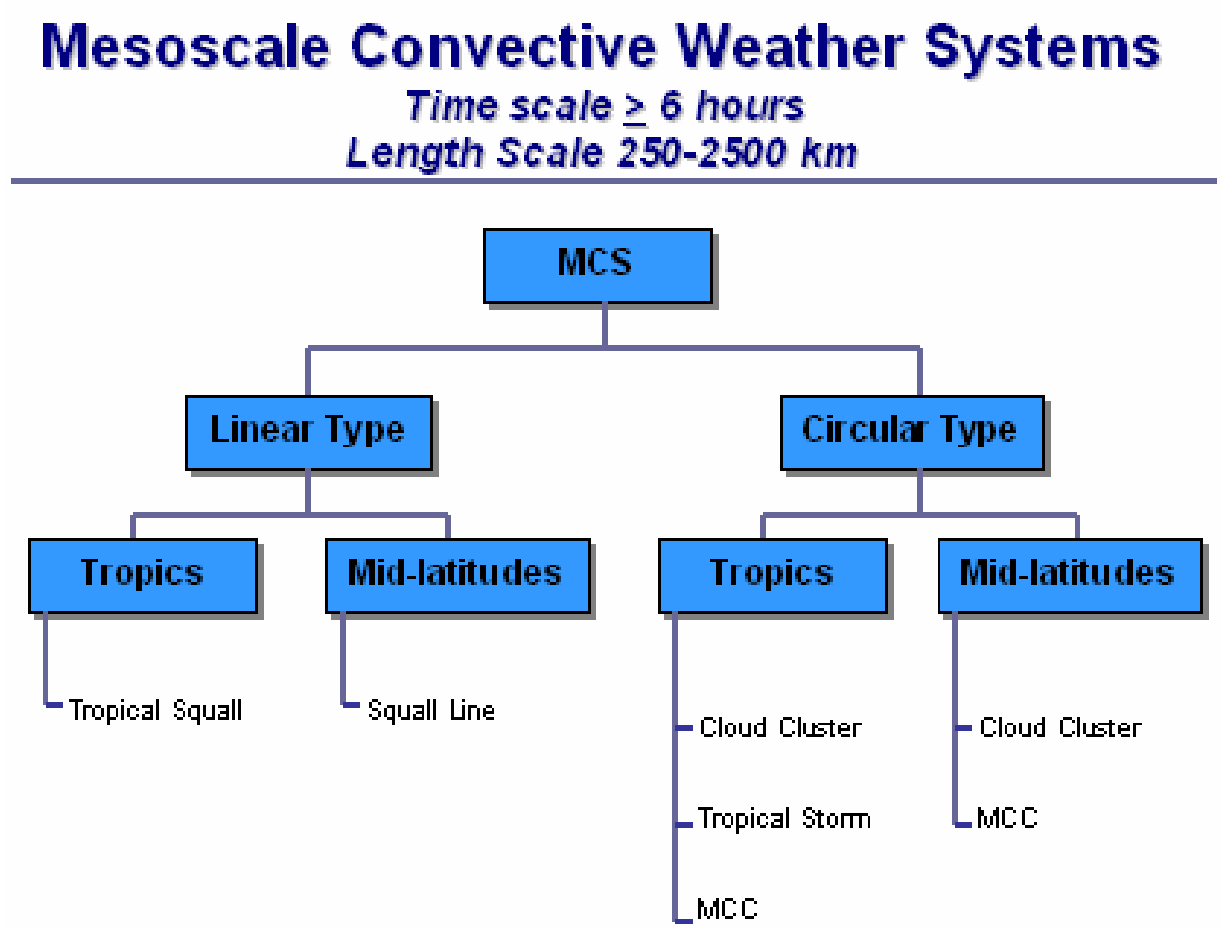

Figure 7-3
Schematic of Mesoscale Convective Weather Systems Classification

From Maddox (1980).

7.3 Squall Lines and Mesoscale Convective Systems. There is the potential for confusion when the terms "squall line", "Mesoscale Convective Complex" and "Mesoscale Convective System" are used. (See the discussion of Doswell (2001) as applied to this subject.) In summary, the term "squall line" was originally applied to the cold front and associated with gusty winds. However, the term now applies to linear convective storm systems or almost any thunderstorm line. With this organization the convective elements interact and often have a common cold pool and outflow (gust front) boundary. The initiation mechanism is often a synoptic or mesoscale boundary such as a dryline, trough, or front. Gaps between adjacent convective elements often fill in to form a nearly two dimensional line of storms (a quasi linear convective system) that may or may not be severe. This is especially true when environmental shear profiles are oriented more parallel to the line orientation, thus encouraging storms that interact or seed and overlap adjacent storms. The definition for the MCC was originally based upon infrared (IR) satellite imagery (Maddox 1980). Maddox chose the largest, most circular, and longest-lasting systems for study. Certain aerial coverage criteria, a duration criterion, and a shape criterion were to be satisfied in order to be labeled a MCC. Essentially, the system's cold cloud shield must surpass a size threshold, persist for at least 6 hours, and must be characterized by a circular shape. Now the entire class of mesoscale systems observed by IR, whether linear or quasi-circular, have come to be termed Mesoscale Convective Systems (Zipser 1982). Almost any squall line, especially those with large mesoscale rain areas are MCSs. Examples of squall lines with large trailing regions of stratiform precipitation have been summarized in conceptual models by Houze et al. (1989) (Figure 7-4), Kessinger et al. (1983), and Parker and Johnson (2000, 2004c) (Figure 7-5).

Conceptual models of squall lines and the MCS have evolved over the years based on studies from higher-resolution satellite, radar, and surface observations. The MCS classification continues to develop from relatively recent studies of convective systems using satellite and radar information, as well as comprehensive field programs such as BAMEX (Davis et al. 2004; Parker and Johnson 2004a, b, c; Wakimoto 2004). There are many convective systems that could be considered as both MCSs and/or squall lines. In fact, linear squall lines are considered as a phase in the development of many MCSs by Parker and Johnson (2004a, b, c). Comprehensive studies, such as those above, of the internal dynamics of MCSs and squall lines and the conditions in which they form, are establishing their similarities and differences.

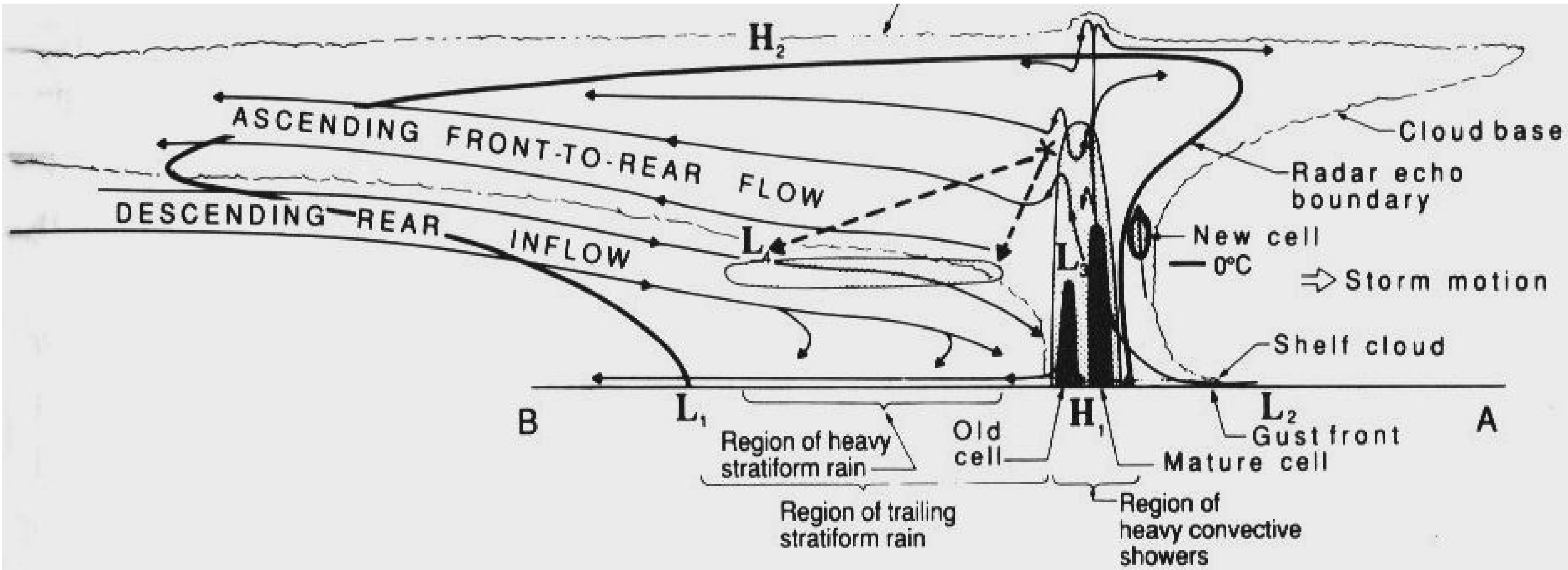

Figure 7-4
Conceptual Model of a Squall-Line System

See the text for a discussion of this model from Houze et al. (1989).

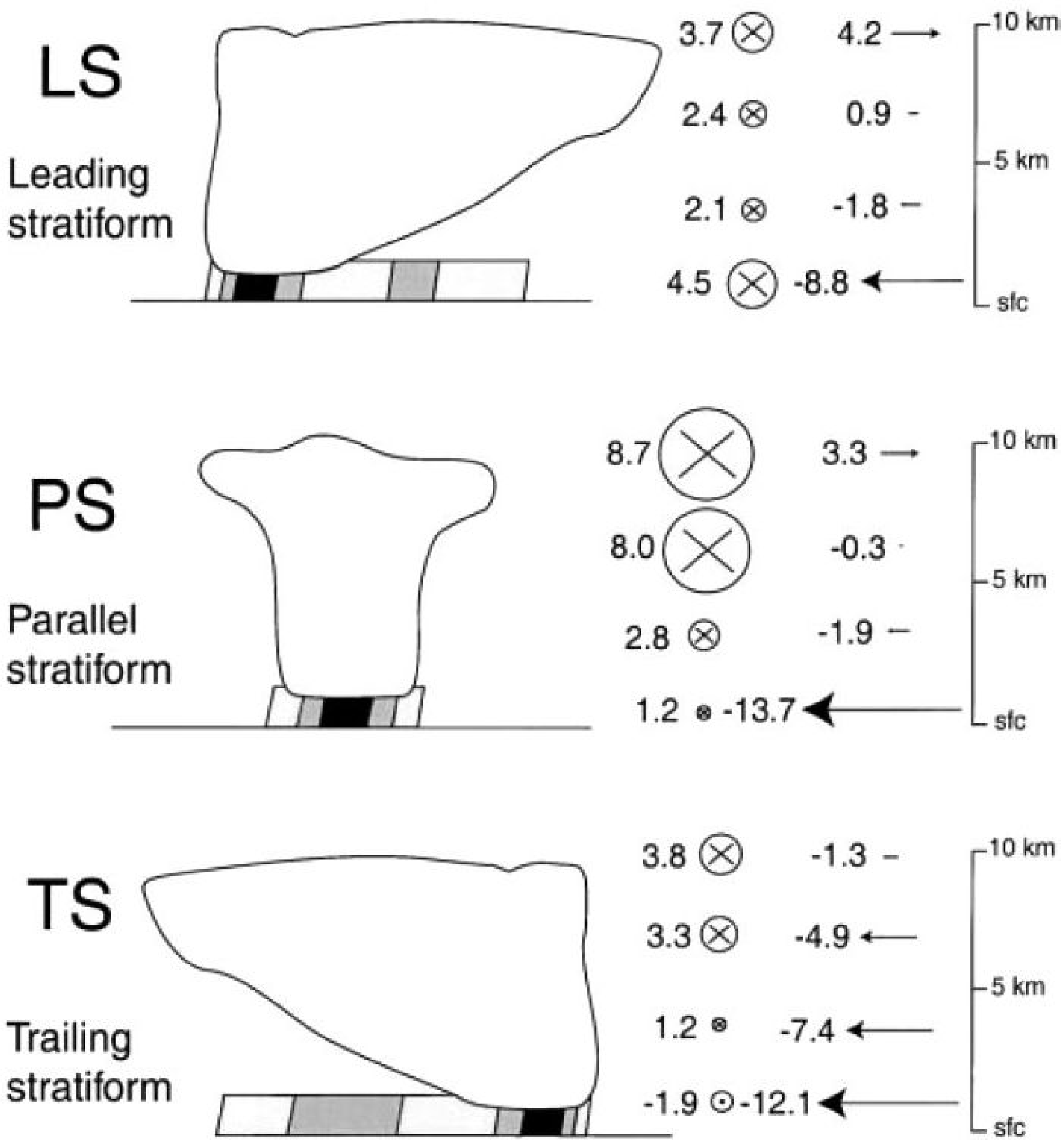

Figure 7-5
A Schematic of Mesoscale Convective System Archtypes

Vertical profiles of layer-mean storm-relative pre-MCS winds for linear MCS classes. Wind vectors are depicted as line-parallel (vectors with arrow) and line-perpendicular (encircled X) components in m s^{-1}. Layers depicted are 0–1, 2–4, 5–8, and 9–10 km (AGL). Typical base scan radar reflectivity patterns (shading) and hypothetical cloud outlines are drawn schematically for reference. MCSs' leading edges are to the right (after Parker and Johnson 2000).

Fritsch and Forbes (2001) point out that there are essentially two classes of MCSs. Type 1 has its origin within a baroclinic system, i.e., an ETC. It results when a mesoscale ribbon of low-level potentially unstable air is forced to ascend in a frontal zone or other region of baroclinic forcing. Type 2 results when the outflow of thunderstorms developing in a more barotropic environment congeal forming a cold pool that interacts with the environmental shear profile in such a way that continuing convection is encouraged and organized along and above the cold pool. One of the dominant characteristics of both types is that they tend to be nocturnal. Often, the nocturnal forcing for the low-level jet downstream from north-south mountain range is important to MCS genesis and maintenance. The surface-based baroclinity facilitates slantwise ascent (warm advection) of the lowest few thousand feet of warm sector air. Continuing ascent saturates this air as it overruns low-level colder more stable air. This process often results in scattered, elevated, deep convection in an along-front direction over a considerable distance which organizes into a "squall line."

Thus, squall lines that occur within extratropical cyclones may initiate as elevated convection in the warm advection area north of the warm front. This same area is often the focus of potential temperature ridges, (a warm and moist tongue) accompanied by a low-level jet (Johns and Hirt 1987; Johns and Doswell 1992). These same authors also addressed those squall lines that are most often located in the warm sector, where the air mass is most unstable. As indicated, a common initiating mechanism is convergence along fronts or discontinuities. Once formed, the squall line provides its own propagating mechanism in the form of convergence along the cold pool and gust front, which maintains ascent into existing updrafts and initiates convection ahead of storms.

Both squall lines (mid-latitude and tropical) and Mesoscale Convective Systems contain multicell characteristics (e.g., cells developing along the leading edge of the line and moving rearward into the large stratiform rain regions). Some distinction is needed in the two classes (of MCS and squall line) to account for the unique three-dimensional attributes often found in MCSs. Some of the MCSs' unique nature of storm structure is based on the environmental conditions and longevity that tend to influence evolution of these large convective systems. These are examined in detail in COMET's web-based instructional component, Mesoscale Convective Systems: Squall Lines and Bow Echoes, available at: http://meted.ucar.edu/convectn/mcs/index.htm. The COMET MCS web module also explains the development of MCSs from initiation to mature phase.

Two of the more widely accepted conceptual models of the complex flow structure for squall lines are from Houze et al. (1989); (see Figure 7-4) and Biggerstaff and Houze (1991).

In the Houze et al. (1989) model of a mature MCS, development of the Rear-Inflow Jet (RIJ) is attributed to mid-level mesoscale areas of low pressure (labeled L3 & L4). The mesolow "L3," which forms immediately behind the leading line convection, is a hydrostatically-induced negative pressure perturbation that develops under the upshear tilted warm convective updrafts and above the evaporatively cooled downdrafts. Mid-level mesolow "L4" forms in the stratiform region in between the warm buoyant air which gets pulled rearward past the cool and the dry descending air flow. Although MCSs develop in a number of ways, all mature systems eventually develop convective regions and stratiform precipitation regions to some degree. The eventual MCS type is determined to a large extent by the environmental wind and deep layer shear conditions in which it develops and the strength of the system's cold pool. Parker and Johnson (2000) studied MCS types and determined the distribution of precipitation and stratiform region shapes were largely a result of mean storm-relative winds (Figure 7-5). The speed and direction of the environmental mid- and upper-level winds relative to the system's motion affect the resulting evolution of the MCS. Thus, storm- (or system-) relative wind fields are critical to the evolution and movement of multicell systems. According to their studies, Parker and Johnson (2000) found MCSs evolve into three major archetypes: 1) trailing stratiform, 2) leading stratiform and 3) parallel stratiform. The main distinction arises from storm-relative flow fields. The leading stratiform precipitation MCS archetype (also see Parker and Johnson 2004a, b), which is typically slower-moving than trailing stratiform systems, was characterized by stronger mid- and upper-level storm-relative flow (often described as rear-to-front flow) than any of the other types (Figure 7-5). The trailing stratiform MCS type has a sloped front-to rear flow produced by stronger system-relative flow.

These multicell storms may consist solely of simple ordinary cells, or they may also contain embedded supercells. These multicell storm systems contain a wide variety of configurations and multiple mechanisms may exist for determining their movement. These mechanisms include, but are not limited to:

- shear-cold pool interactions,
- low-level convergence,
- instability gradients, and
- three-dimensional boundary interactions.

Some of MCS's unique nature of storm structure is based on the environmental conditions that tend to influence evolution and longevity of these large convective systems. These are examined in detail in COMET's web based instructional component, Mesoscale Convective Systems: Squall Lines and Bow Echoes, available at this web address:
http://meted.ucar.edu/convectn/mcs/index.htm. The module is highly recommended reading to complement this Handbook. However, of equal importance is some of the more recent work that has emphasized not only the low-level shear interaction with the cold pool, but also the importance of deep-layer shear (Congilio et al. 2004a, b).

Derecho events, as we will see, are defined as a series of damaging wind episodes, Johns and Hirt 1987), which are the fastest moving multicell systems, can last from 2 to over 20 hours and can travel across multiple County Warning Areas if downstream instability remains sufficient. Additionally, those MCSs/squall lines containing embedded supercells are very often associated with high-end (extreme but non-tornadic) damaging wind events (Miller and Johns 2000; Miller et al. 2002). Those events are associated with the supercells themselves.

A wave in a line of thunderstorms that is sometimes associated with one or more bow echoes is called a Line Echo Wave Pattern (LEWP) (Figure 7-6). Nolen (1959) found that these echo structures were often associated with damaging winds and other potential servere weather. Multiple bow echoes within a squall line may sometimes result in a LEWP. Many features of bow echo evolution which cause a typical LEWP structure (such as the rotating comma head and the cyclonic/anticyclonic rotating vortices) are based on the conceptual model from Fujita (1978), (Figure 7-7).

Fujita found that the initial echo started as a strong isolated cell or a small line of cells. The initial cells then evolved into a quasi-symmetric bow-shaped segment of cells over a period of an hour or two, and eventually into a comma-shaped echo over several hours. More recently, Burke and Schultz (2004) documented several other modes of bow-shaped echo development such as the latter stages of some supercells.

A distinction should be made between a squall line that contains closely spaced interactive cells with nearly continuous precipitation throughout its length and one consisting of a line of isolated or quasi-isolated storms. These two types differ both in appearance and other characteristics. It is not uncommon for a line of isolated cells with severe weather to evolve into a solid line by a progressive filling of gaps in the line. This is typically the case when the deep layer shear vector is oriented largely parallel to the line. In the case where the initially isolated cells were tornadic, this evolution often signals the end of tornadic activity, although damaging straight-line winds, hail, and heavy rains may persist. (Note, however, as explained previously, squall lines in the form of bows or LEWPs and those containing embedded supercells may still be significantly tornadic despite being members of quasi linear convective systems [QLCS].) Tornadic activity frequently, but not always, shifts to isolated cells ahead of the line or cells that occur at the southern or southwestern end of the squall line and/or on the northern end of a gap in a line. Existing lines sometime increase in length by new cell development on the southern or western end of the line.

Updrafts often form a nearly continuous curtain along the advancing edge of the QLCS echo. Downdrafts form in the precipitation echo to the rear of the leading updrafts. That portion of the line often with the most intense gust front and updrafts is identified by a strong reflectivity gradient at low altitude, echo overhang and related forward WER, and a shift of echo top from over the storm core to along the leading edge of the line. Sometimes the surface gust front surges ahead of the leading edge of the echo and, if close enough to the radar, can be observed as a thin line echo (Figure 7-6).

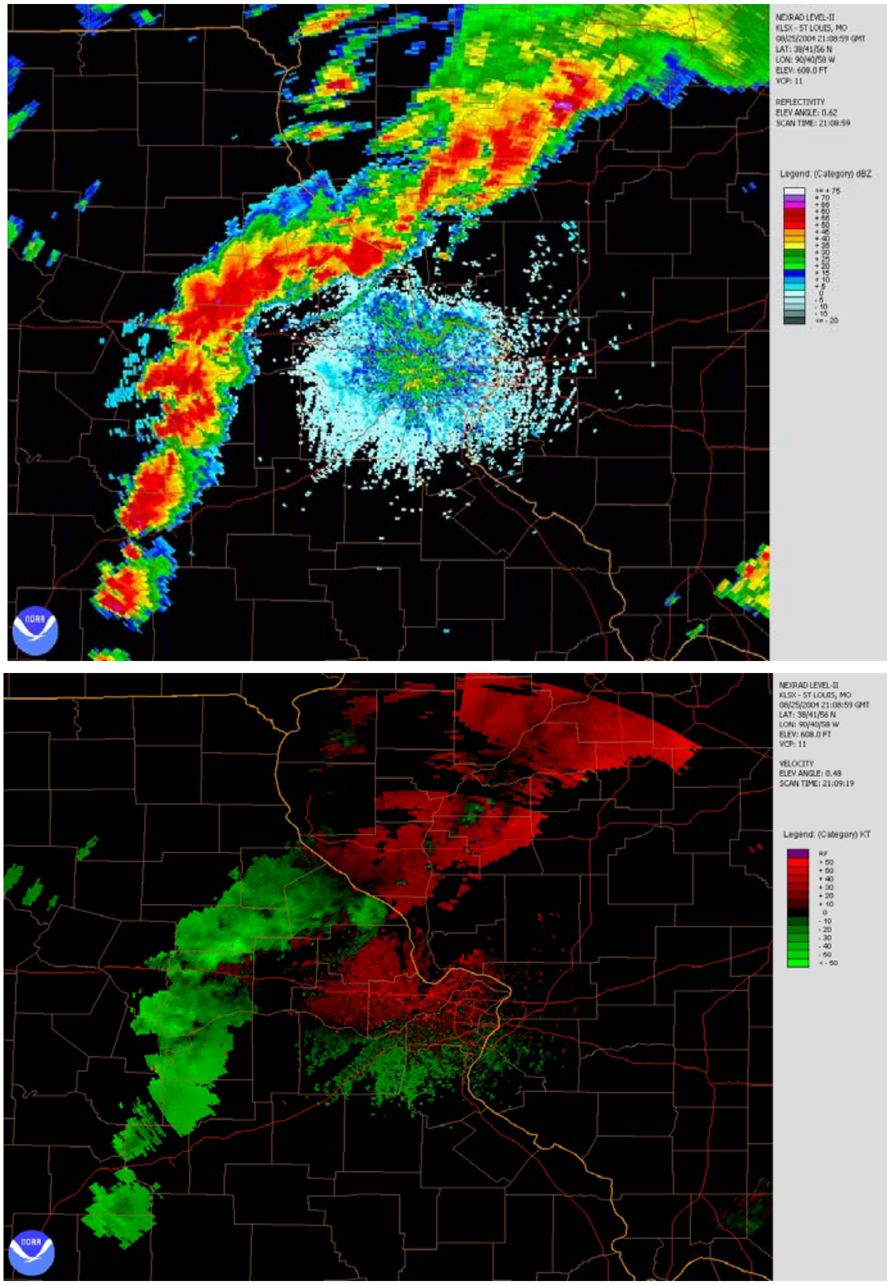

Figure 7-6
Line Echo Wave Pattern

St. Louis, MO WSR-88D Reflectivity product (top) and Mean Radial Velocity product (bottom), both at 0.5° elevation, and at 21:08 UTC on 25 August 2004 (NCDC NEXRAD Viewer graphic). A squall line in the form of a Line Echo Wave Pattern (LEWP) is north and west of St. Louis. A gust front can be seen northwest of the radar in both reflectivity and velocity imagery.

Rear-Inflow Jets (RIJs) are common with large QLCSs or MCSs. However, numerical simulations suggest the RIJs do not descend in the most severe squall lines (Weisman 1992). According to Weisman (1992), most squall lines become upshear-tilted as the cold pool dominates environmental shear and the non-descending RIJ restores balance, allowing the squall line updraft to remain nearly vertically erect for longer periods of time. Non-descending RIJs are found in environments where deep layer shear and conditional available potential energy (CAPE) are high.

A radar signature which is often associated with the RIJ and with high winds and tornadoes is the Mid-Altitude Radial Convergence Signature (MARC). This is a signature very similar to the Deep Convergence Zone, or DCZ, identified by Lemon and Burgess (1993) and Lemon and Parker (1998) that is also found to be associated with strong and damaging surface winds. However, those authors emphasized the extreme depth and convergence sometimes associated with the MARC. Observations of a MARC have been noted by Przybylinski (1998) as a precursor to the descent of the elevated RIJ. Enhanced velocity differentials (areas of strong convergence) are often located just downwind of high reflectivity cores along the leading edge of the convective line. Persistent areas of MARC greater than 25 ms^{-1} at 3-5 km AGL can sometimes provide lead time for the first report of wind damage (often before a well-defined bow echo with bookend vortex develops). On either end of mature squall lines and flanking the RIJ, can sometimes be found "book-end" vortices (and sometimes supercells), cyclonic on the north end and anticyclonic on the south end. Squall line segments exhibiting line-end vortices and a localized RIJ in between the vortices and directed toward the leading edge are often called bow echoes based on their bowing configuration (Figure 7-8). Bow echoes intensify the RIJ between the vortices, often leading to localized areas of maximum wind damage. Small tornadoes may occur just to the left of the maximum wind in an RIJ and with leading edge mesocyclones given enough low-level helicity and instability in the environment. The line-end vortices in bow echoes (Figure 7-7 and Figure 7-8) develop in one of two ways; by either tilting negative storm induced vorticity at the top end of the cold pool from the storm updraft, and/or by tilting positive environmental vorticity downward by the downdraft in the back end of a bow echo. More will be said about bow echoes and these line-end vortices shortly.

Bow echoes and RIJs are sometimes associated with Derechos. Johns and Hirt (1987) studied warm-season Derechos. They defined the Derecho as:

1). A concentrated area of convectively induced wind damage and/or gusts >50kts (25ms^{-1}) that has a major axis length of at least 250 nm (463 km).

2). Reports must show a pattern of chronological progression.

3). At least 3 reports of convective gusts >65kts (33ms^{-1}) and/or F1 intensity damage. These 3 reports must be separated by 40 nm (74 km) or more.

4). No more than 3 hours can elapse between successive wind damage (gust) events.

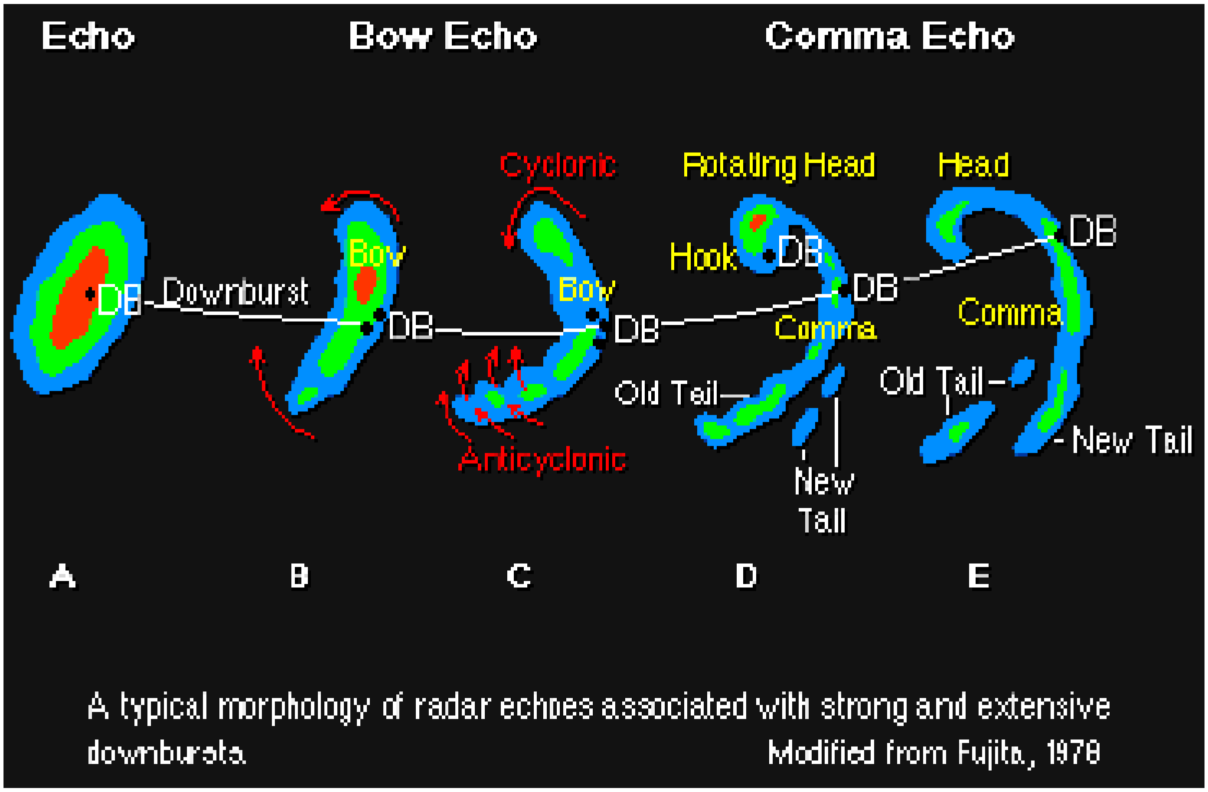

Figure 7-7
Conceptual Bow Echo Evolution

Conceptual model of a bow echo evolution. Adapted from Fujita (1978) and COMET (1999).

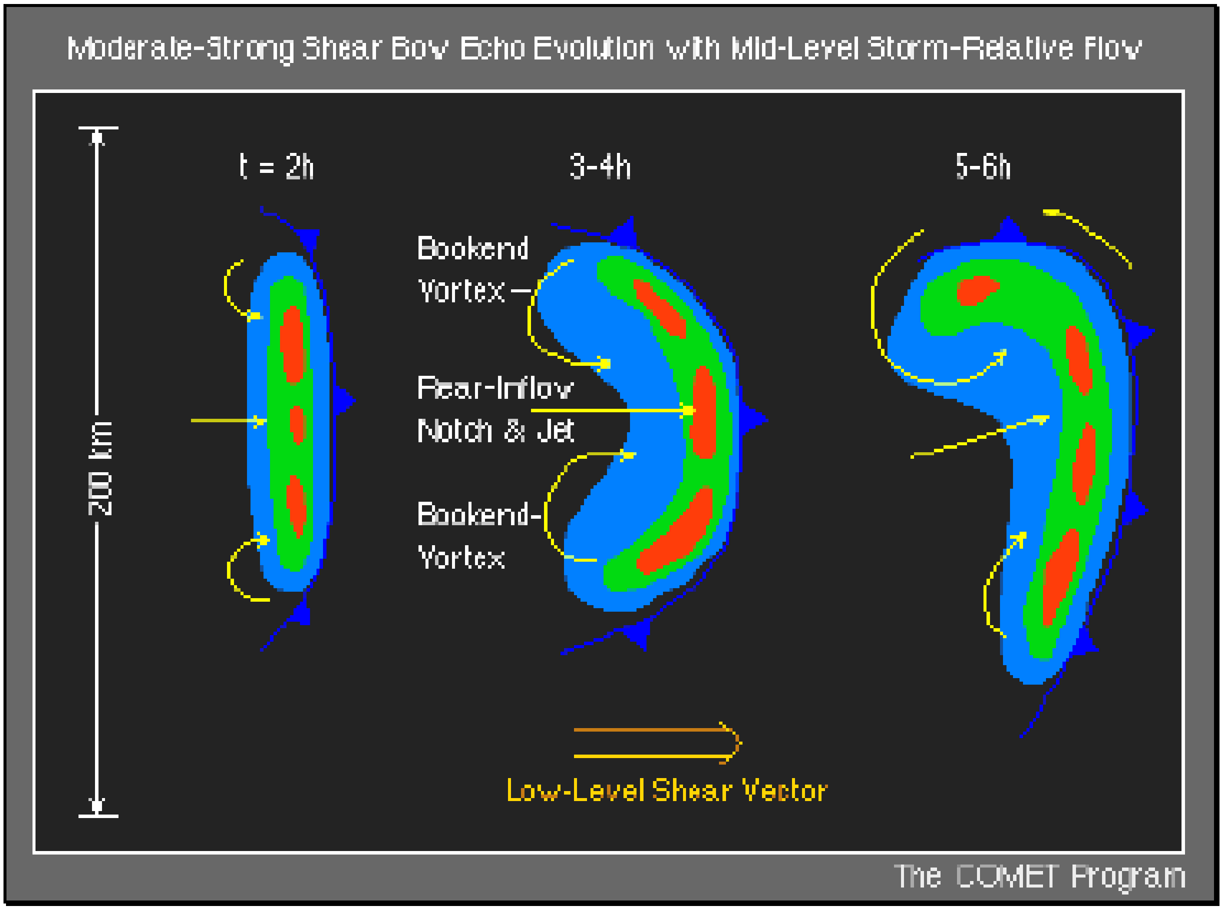

Figure 7-8
Conceptual Bow Echo Model

Conceptual model of a strong bow echo evolution showing bookend vortices and development of a Rear-Inflow Notch (RIJ). From COMET (1999).

They found that Derecho environments were characterized by copious moisture at low levels and extreme convective instability. However, in synoptically forced cases, lesser instability accompanied the “strong” 500 mb shortwave troughs in their data set. Similarly, Johns et al. (1990) examined 14 very intense Derechos during the months of June and July and found that CAPE values were generally greater than 2400 J/kg near the genesis region, but increased to an average CAPE maximum of 4500 J/kg as the convective system moved eastward. In fact, the studies by Miller and Johns, 2000, and Miller et al. 2002 found that those high-end Derechos occurred within the same types of environments associated with outbreaks of tornadic storms (strong CAPE and strong deep-layer shear).

Evans and Doswell (2001) also studied CAPE distributions in squall lines (via proximity soundings) and found a much greater range of values for Derecho events. They found that in most cases which were weakly-forced, the instability (and CAPE) were generally larger than in those cases where the forcing was “strong” (SF). For SF, there were a number of Derecho systems that developed and persisted in environments with low values of CAPE. A few Derechos developed and persisted within regions of conditionally stable surface air. Thus, squall lines have been observed over a wide range of environmental CAPE (and vertical wind shear). For any given CAPE, the intensity and longevity of linear convective systems seem to increase with increasing synoptic scale forcing, which includes depth and strength of the vertical wind shear.

Bluestein and Jain (1985) studied squall lines in Oklahoma and found that the magnitude of the vertical wind shear on average was stronger for severe lines than for the non-severe lines. In their study, the average CAPE for severe lines was significantly larger than for the non-severe lines (2260 J/kg versus 1372 J/kg), which agrees with other studies.

While we have omitted other discussion that can be found elsewhere (see IC 5.7, WDTB web site) we can summarize the relationship between CAPE and shear. The intensity and longevity of squall lines and bow echoes occur within a wide range of environmental conditions and shear/buoyancy parameters. As in supercell environments, for stronger synoptic forcing, deep layer shear is usually stronger and CAPE is smaller. The converse holds true as well; in weaker synoptic forcing, higher CAPE and Downdraft CAPE (DCAPE) are necessary to maintain the strong winds at the surface. Thus, there is a greater dependence, in weak (0-6 km) flow situations, on strong downdrafts and cold pools for maintaining severe surface winds.

Given the same buoyancy for updrafts and cold pools, shear can modulate the intensity of the RIJ. According to numerical simulations, as shear increases, the updraft along the leading edge becomes more erect and stronger. More heat is pumped into the anvil just behind the leading edge causing a stronger hydrostatic low in the mid-levels. The more intense precipitation from the stronger updraft is hypothesized to create a stronger cold pool and gust front as well.

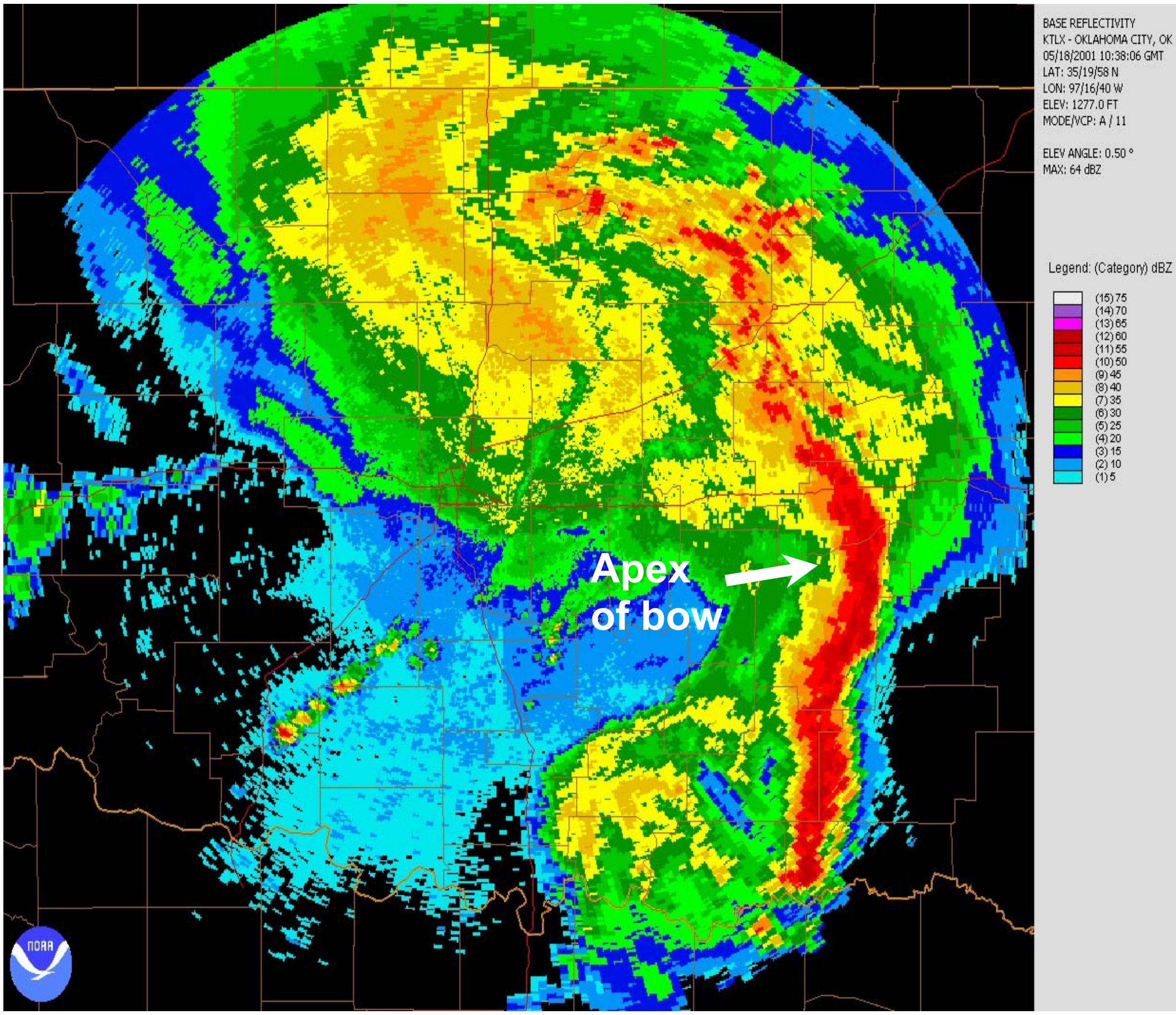

Figure 7-9
Reflectivity Image of a Bow Echo

Oklahoma City, OK WSR-88D 0.5° Reflectivity product at 10:38 UTC on 18 May 2001 (NCDC NEXRAD Viewer graphic). This image is of a bow echo in Eastern Oklahoma as annotated.

While the role of vertical wind shear in the strength, structure, and maintenance of MCSs has been examined by many, much of this work focuses on the interaction of the low-level shear with the circulation induced by the cold thunderstorm outflow (see a summary in Weisman and Rotunno 2004). However, the relative importance of upper-level wind shear has been neglected until more recently. Coniglio et al. (2004a, b), via simulations, as well as observations, has shown convincing evidence that deep layer shear helps to organize and maintain the MCS and the Derecho associated MCS, especially in situations involving weak forcing and the lack of a strong low-level jet. Furthermore, this work also helps explain the demise in these systems when wind shear in the 7 to 9 km AGL range weakens.

When the squall line is trailed by stratiform precipitation, the first indication that a bow echo is about to develop is sometimes the erosion of the back edge of the adjacent stratiform echo, accompanied by the strong velocities of the RIJ directed toward the forward convective-line flank. Figure 7-9 is a mature squall line with an embedded, developing bow echo. Some line echoes evolve into the comma shape that shows rotation within the "book end" vortices.

While the presence of bow echoes and LEWPs are often used by the meteorological practioner as a severe weather indicator, this does not guarantee that a severe storm is imminent. Confirmation can be obtained via the updraft flank signatures of the Weak Echo Region (WER) and the Bounded Weak Echo Region (BWER) associated with the mid-level echo overhang, strong low-level reflectivity gradients, and the displaced echo top are all signatures associated with intense updrafts (e.g., Lemon 1980) and severe weather. This is the case for nearly all severe storms that are severe by virtue of intense updrafts, even with squall lines (Figure 7-10). The radial velocity data from low altitude scans sufficiently close to the radar can be used to estimate the intensity of surface winds associated with thunderstorm outflows and to determine if mesocyclone development accompanies storms within the line. Further, at longer ranges, mid-level convergence identified in radial velocity fields and associated with the Deep Convergence Zone, or DCZ, (Lemon and Burgess 1993; Lemon and Parker 1998) and the related Mid-Altitude Radial Convergence (MARC) (Schmocker et. al. 1996) can be used to infer strong downdrafts and associated strong, damaging surface winds.

7.4 <u>Storm Development on Airmass Boundaries</u>. New convective cells commonly develop along gust fronts, outflow boundaries, mesoscale and synoptic scale boundaries, boundaries of all types. A large fraction of non-frontal thunderstorms form on these boundaries and at the intersection of existing boundaries as detected on visible satellite photographs. These boundaries are most often associated with density discontinuities. The boundaries can often be detected on radar and are commonly known as thin or fine lines. However, it should be noted that the effective range for boundary layer probing is limited by the Earth's curvature (radar horizon) and the finite beam width. Reflectivity is enhanced not only by turbulent mixing of warm and cool air along the discontinuity, but by insects carried into the boundary by the airflow as well as their predators, birds (Figure 7-11). At times, migratory birds will use the wind-flow behind fronts to aid them in their migratory journeys. This can create significant echo return behind the boundary, as well, and is also seen in Figure 7-11. As the front passes, the birds at the surface will take to flight. Clouds (containing precipitation size hydrometeors) need not be present as the echoes are from refractive index perturbations associated with the mixing and the insects and birds themselves.

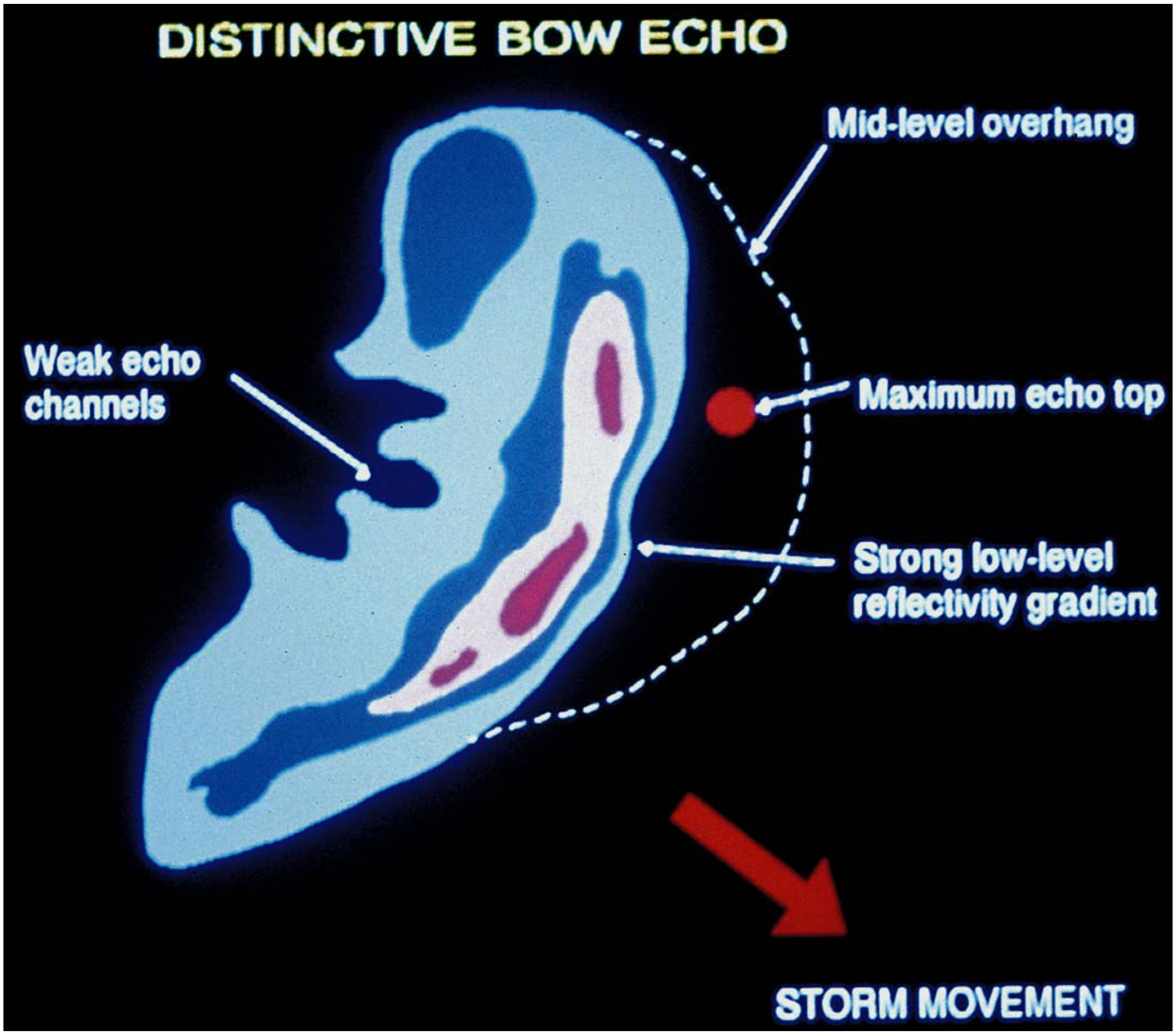

Figure 7-10
Schematic Diagram of a Distinctive Bow Echo

Features associated with the strong updraft along the leading edge of the Distinctive Bow Echo including the mid-level echo overhang, displaced echo top, and strong low-level reflectivity gradient. (After Przybylinski and Gery 1983).

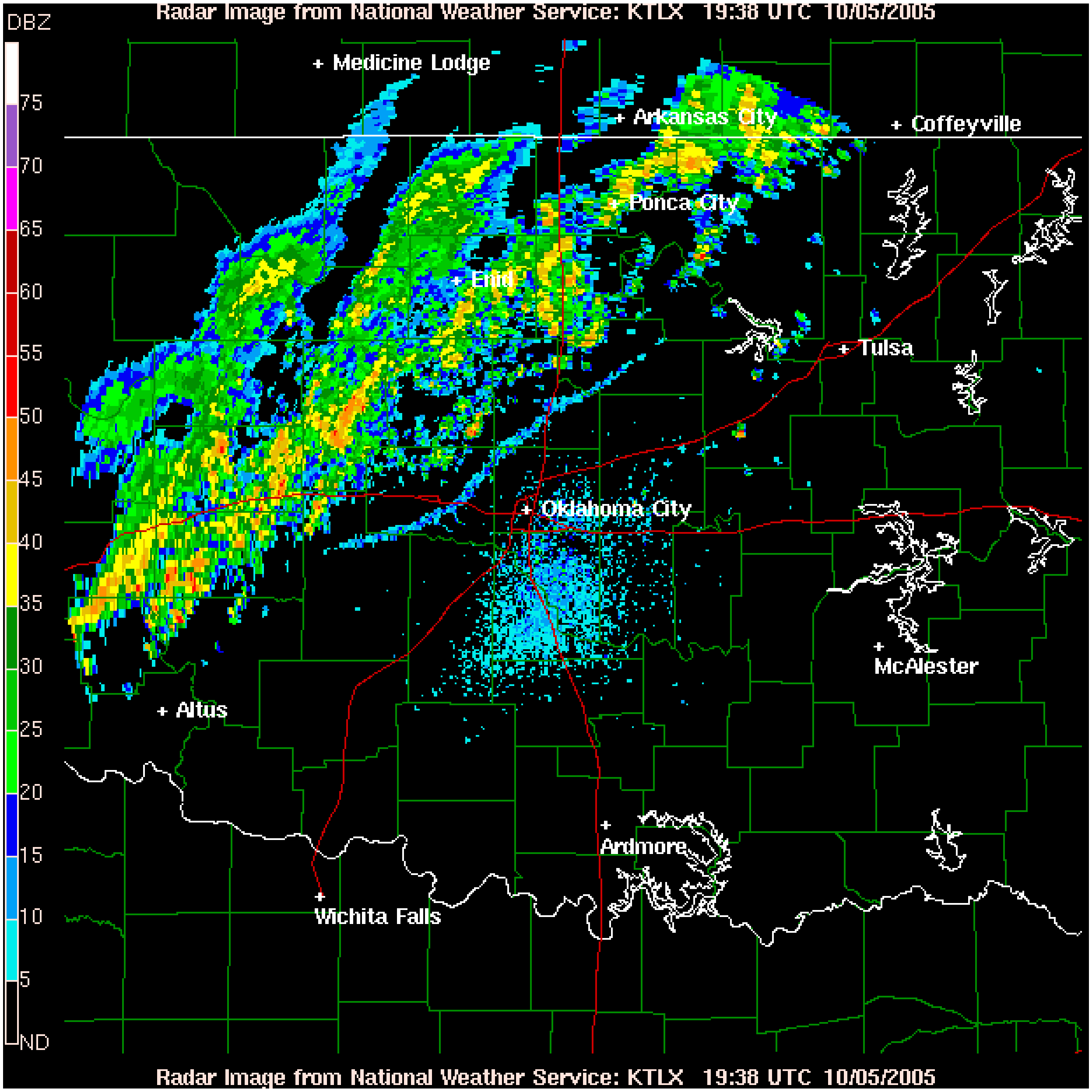

Figure 7-11
Base Reflectivity Product with a Cold Front

A cold front approaching the Oklahoma City, OK WSR-88D at 19:38 UTC on 5 October 2005 is shown on this 0.5° Reflectivity product. The cold front is the northeast – southwest oriented line (predominantely blue color/reflectivities less than 20 dbZ) northwest of the radar and southeast of the broader area of convection. This image was taken from the NWS Radar Image web page.

Thunderstorm development can, in many cases, be anticipated by identifying the intersection of boundaries tracked by radar or by enhanced reflectivity along these lines. In some cases, boundaries are not traceable to thunderstorms or other causes and may not be accompanied by density gradients. WSR-88D velocity data can be used to determine if such lines are accompanied by wind shifts and convergence that may trigger storms.

Also, general lifting of air above a front can sometimes be estimated from Doppler data using the VAD algorithm (Part C, Chapter 3, of this Handbook).

Once these boundaries have passed a location and sufficient precipitation exists behind the boundary, the VAD Wind Profile (VWP) can be applied to monitor the nature of the thermal advection, the depth of cold air, numerical model performance and the vertical depth of echo (precipitation, and in clear air situations, non-precipitation particles) (Figure 7-12). When convection generated in association with boundaries surrounds or is nearby the radar, often the VWP winds will not be representative of the environment. However, the VWP seen in Figure 7-12 was made by a radar located north of a warm front and within a developing ETC. Note that, in this case, the depth of the cold air can be determined beneath the wind shift at ~5,000 ft (~1500 m). Notice, too, that in the colder air beneath the frontal surface, winds are from a northeasterly direction. Within the frontal zone, winds veer in direction to southerly and then to the southwest. Stratiform precipitation echo extends to ~ 24,000 ft (~7300 m) ahead of an advancing mid-level short wave.

The subject of the Morphology of Large-Scale Precipitating Weather Systems is admittedly broad and is only partially discussed here. The reader may wish a more detailed treatise and is urged to obtain text books on the subject (e.g., Bluestein 1992; Shapiro and Gronas 1999; Carlson 1998). The following Internet and references are also available:

- Mesoscale Meteorology Severe Convection II: Mesoscale Convective Systems – Bibliography:

  http://meted.ucar.edu/mesoprim/severe2/print_version/_p_9.0Bibliography.htm.

- Cold Pool/Shear Interactions in Mesoscale Convective Systems:

  http://www.hprcc.unl.edu/nebraska/pool-shear.html,

- References:

  http://www.hprcc.unl.edu/nebraska/references.html.

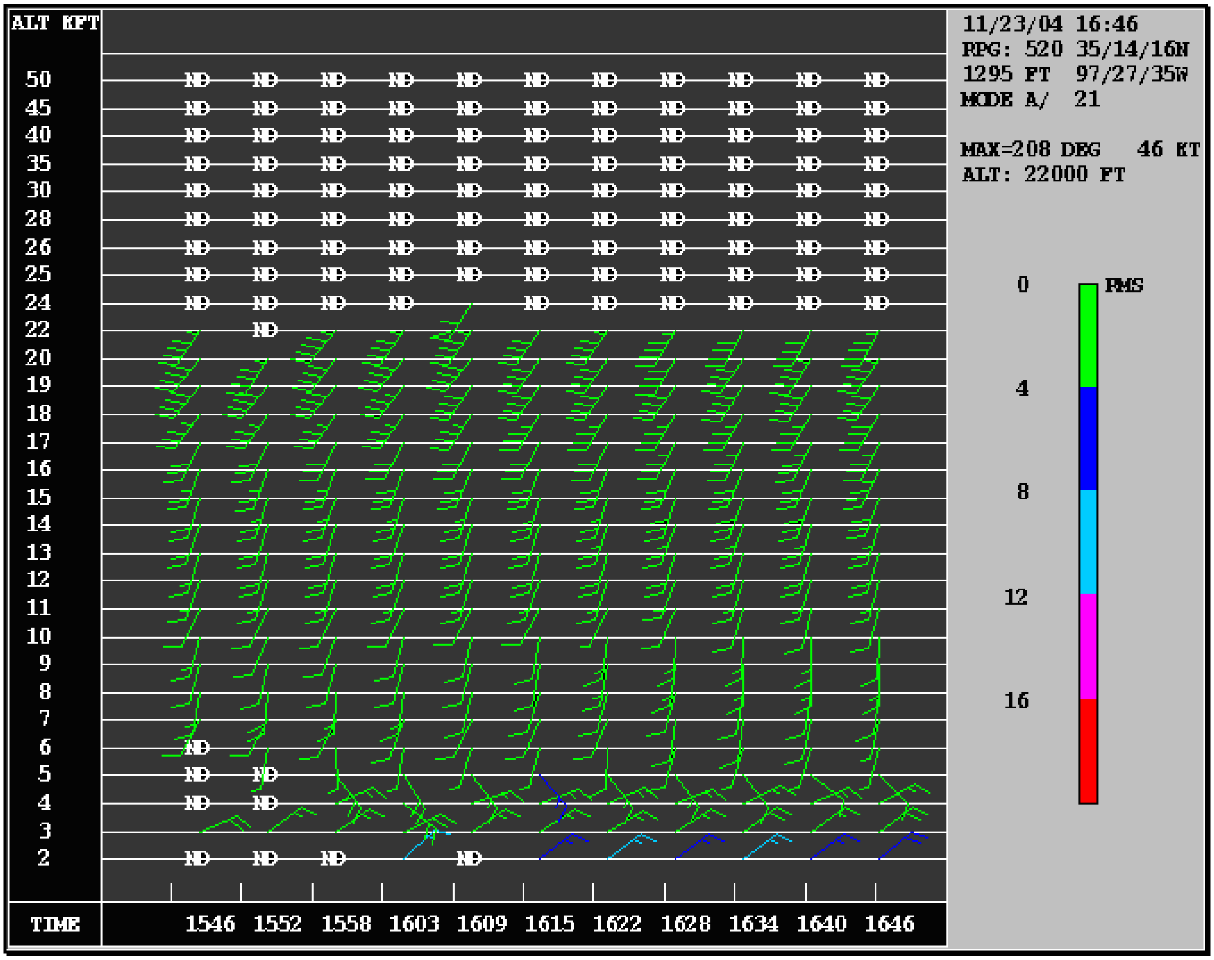

Figure 7-12
VAD Wind Profile

This VWP product was collected by the Wichita, KS WSR-88D at 16:52 UTC on 23 November 2004 (NCDC NEXRAD Viewer graphic). Note the wind shift from northeast at 20 kts (10 ms-^{1}) at 4,000 ft (~1200 m) to south at 5 kts (2.5 ms^{-1}) at 6,000 ft (~1800 m). This wind shift marks the frontal surface near 5,000 ft (~1500 m).

REFERENCES

Atlas, D. (Ed), 1990: *Radar in Meteorology*. Amer. Meteor. Soc., Boston, MA., 773 pp.

Bluestein, H. B., 1992: *Synoptic-Dynamic Meteorology in Midlatitudes*, Vol. I and II, Oxford University Press, 1015 pp.

Bluestein, H. B. and M. H. Jain, 1985: Formation of mesoscale lines of precipitation: Severe squall lines in Oklahoma during the spring. *J. Atmos. Sci*., **42**, 1711-1732.

Burke, P. C. and D. M. Schultz, 2004: A 4-yr climatology of cold-season bow echoes over the continental United States, *Wea. Forecasting*, **19**, 1064-1071.

Carlson, T. N., 1998: Mid-Latitude Weather Systems. Amer. Meteor. Soc., Boston, MA, 507 pp.

COMET, Mesoscale Convective Systems: Squall lines and Bow Echoes, 1999, Cooperative Program for Operational Meteorology, Education and Training, Distance Learning Program. http://www.meted.ucar.edu/convectn/mcs/.

Coniglio, M. C., D. J. Stensrud, and L. W. Wicker, 2004: How mid- and upper-level shear can promote organized convective systems. Preprints, *22nd Conf. on Severe Local Storms,* Zurich, Amer. Meteor. Soc., paper 10.5.

Coniglio, M. C., D. J. Stensrud, and M. B. Richman, 2004: An observational study of derecho-producing convective systems. *Wea. Forecasting*, **19**, 320-337.

Doswell, C. A. III, 2001: Severe Convective Storms – An overview, *Severe Convective Storms*, *Meteor. Monogr*., **50**, C. A. Doswell (Ed.), Amer. Meteor. Soc., Boston, MA, 561 pp.

Evans, J., and C.A. Doswell III, 2001: Examination of derecho environments using proximity soundings. *Wea. Forecasting*, **16**, 329-342.

Fritsch, J. M., and G. S. Forbes, 2001: Mesoscale convective systems. *Severe Convective Storms, Meteor. Monogr.,* No. **50**, Amer. Meteor. Soc., 323–357.

Fujita, T. T., 1978: Manual of downburst identification for Project NIMROD. SMRP Res. Pap. 156, University of Chicago, 104 pp.

Hane, C. E., 1984: Extratropical Squall Lines and Rainbands. AMS Intensive Course on Mesoscale Meteorology and Forecasting, Boulder, CO.

Houze, R. A., Jr., S. A. Rutledge, M. I. Biggerstaff, and B. F. Smull, 1989: Interpretation of Doppler weather radar displays in midlatitude mesoscale convective systems. *Bull. Amer. Meteor. Soc*., **70**, 608-619.

Johns, R. H., and W. D. Hirt, 1987: Derechos: Widespread Convectively Induced Windstorms. *Wea. Forecasting*, **2**, 32-49.

Johns, R. H., K. W. Howard, and R. A. Maddox, 1990: Conditions Associated with Long-Lived Derechos - An Examination of the Large-Scale Environment. Preprints, *16th Conf. on Severe Local Storms*, Kananaskis Park, AB, Canada, Amer. Meteor. Soc., 408-412.

Jorgensen, D., 1982: The Organization and Structure of Hurricane Convective Bands with Applications to NEXRAD. *NEXRAD Doppler Radar Symposium/Workshop*, Univ. of Oklahoma, Norman, OK, pp. 68-81.

Kessinger, C. J., P. S. Ray, and C. E. Hane, 1983: *An Oklahoma Squall Line: A Multiscale Observational and Numerical Study,* Cooperative Institute for Mesoscale Meteorological Studies Report No. 34, 211 pp.

Kessinger, C. J., P. S. Ray, and C. E. Hane, 1987: The Oklahoma squall line of 19 May 1977. Part I: A multiple Doppler analysis of convective and stratiform structure. *J. Atmos. Sci*., **44**, 2840-2864.

Koscielny, A. J., R. J. Doviak, and R. M. Rabin, 1982: Statistical considerations in the estimation of divergence from single-Doppler radar and applications to pre-storm boundary layer observations. *J. Appl. Meteor*., **21,** 197-210.

Lemon, L. R., 1980: Severe thunderstorm radar identification techniques and warning criteria. NOAA Tech. Memo. NWS NSSFC-3, 60 pp.

Lemon, L. R., D. W. Burgess, 1993: Supercell associated deep convergence zone revealed by a WSR-88D. Preprints, *26th Inter. Conf. on Radar Meteorology*, Norman, OK, Amer. Meteor. Soc., 206-208.

Lemon, L. R., and S. Parker, 1996: The Lahoma storm deep convergence zone: Its characteristics and role in storm dynamics and severity. Preprints, *18th Conf. on Severe Local Storms*, Atlanta, GA, Amer. Meteor. Soc., 70-75.

Maddox, R. A., 1980: Mesoscale convective complexes. *Bull. Amer. Meteor. Soc.,* **61,** 1374–1387.

Maddox, R. A., K. W. Howard, and D. L. Bartels, and D. M. Rodgers, 1986: Mesoscale convective complexes in the middle latitudes. *Mesoscale Meteorology and Forecasting* P. S. Ray, Ed., Amer. Meteor. Soc.

Miller, D.J., and R.H. Johns, 2000: A Detailed Look at Extreme Wind Damage in Derecho Events, Preprints, *20th Conf. on Severe Local Storms*, Orlando, FL, Amer. Meteor. Society, 52-55.

Miller, D.J., D.L. Andra, J.S. Evans and R.H. Johns, 2002: Observations of the 27 May 2001 High-End Derecho Event in Oklahoma, Preprints, *21st Conf. on Severe Local Storms*, San Antonio, TX, Amer. Meteor. Society, 13-16.

Nolen, R. H., 1959: A radar pattern associated with tornadoes. Bull. Amer. Meteor. Soc., 40, 277–279.

Ogura, Y., and M. T. Liou, 1980: The structure of a mid latitude squall line: A Case Study. *J. Atmos. Sci*., **37,** 553-567.

Parker, M.D., and R.H. Johnson, 2004a: Simulated convective lines with leading precipitation. Part I: Governing dynamics. *J. Atmos. Sci.,* **61**, 1637-1655.

Parker, M. D., and R. H. Johnson, 2004b: Simulated convective lines with leading precipitation. Part II: Evolution and maintenance. *J. Atmos. Sci.,* **61**, 1656-1673.

Parker, M. D., and R. H. Johnson, 2004c: Structures and dynamics of quasi-2D mesoscale convective systems. *J. Atmos. Sci*., **61**, 545-567.

Parker, M. D. and R. H. Johnson, 2000: Organizational modes of midlatitude mesoscale convective systems. *Mon. Wea. Rev*., **128**, 3413-3436.

Przybylinski, R. W., and W. J. Gery, 1983: The reliability of the bow echo as an important severe weather signature. Preprints, *13th Conf. On Severe Local Storms*, Tulsa, OK, Amer. Meteor. Soc., 270-273.

Rabin, R. M., D. E. Engles, and A. J. Koscielny, 1987: Applications of a Doppler radar to diagnose a frontal zone prior to thunderstorms. *Mon. Wea. Rev*., **115,** 2674-2686.

Rogers, R. R., 1976: *A Short Course in Cloud Physics*, Pergamon Press, 224 pp.

Schmocker, G. K., R. W. Pryzbylinski, and Y.J. Lyn, 1996: Forecasting the initial onset of damaging downburst winds associated with a mesoscale convective system (MCS) using the mid-altitude radial convergence (MARC) signature**.** Preprints**,** *15th Conf. on Wea. Analysis and Forecasting,* Norfolk, VA, 306-311.

Shapiro, M. A., and S. Grønås, (Ed.), 1999: The Life Cycles of Extratropical Cyclones. Amer. Meteor. Soc. Boston, MA, 359 pp.

Wakimoto, R. M., C. Huaqing, and H. V. Murphey, 2004: The superior, Nebraska supercell during BAMEX. *Bull. Amer. Meteor*. Soc., **85**, 1095-1106.

Weisman, M.L., and R. Rotunno, 2004: "A theory for strong, long-lived squall lines" revisited. *J. Atmos. Sci*., **61**, 361-382.

Wilson, J. W., R. E. Carbone, H. Baynton, and R. J. Serafin, 1980: Operational applications of meteorological Doppler radar. *Bull. Amer. Meteor. Soc.*, **61,** 1154-1168.